



HAL
open science

Synthesis, crystal structure, tropicity and charge transport properties of diindenothienothiophene derivatives

Tanguy Jousselin-Oba, Masashi Mamada, Karen Wright, Jérôme Marrot, Chihaya Adachi, Abderrahim Yassar, Michel Frigoli

► To cite this version:

Tanguy Jousselin-Oba, Masashi Mamada, Karen Wright, Jérôme Marrot, Chihaya Adachi, et al.. Synthesis, crystal structure, tropicity and charge transport properties of diindenothienothiophene derivatives. *Journal of Materials Chemistry C*, In press, 10.1039/D2TC01324J . hal-03663987

HAL Id: hal-03663987

<https://hal.science/hal-03663987>

Submitted on 10 May 2022

HAL is a multi-disciplinary open access archive for the deposit and dissemination of scientific research documents, whether they are published or not. The documents may come from teaching and research institutions in France or abroad, or from public or private research centers.

L'archive ouverte pluridisciplinaire **HAL**, est destinée au dépôt et à la diffusion de documents scientifiques de niveau recherche, publiés ou non, émanant des établissements d'enseignement et de recherche français ou étrangers, des laboratoires publics ou privés.

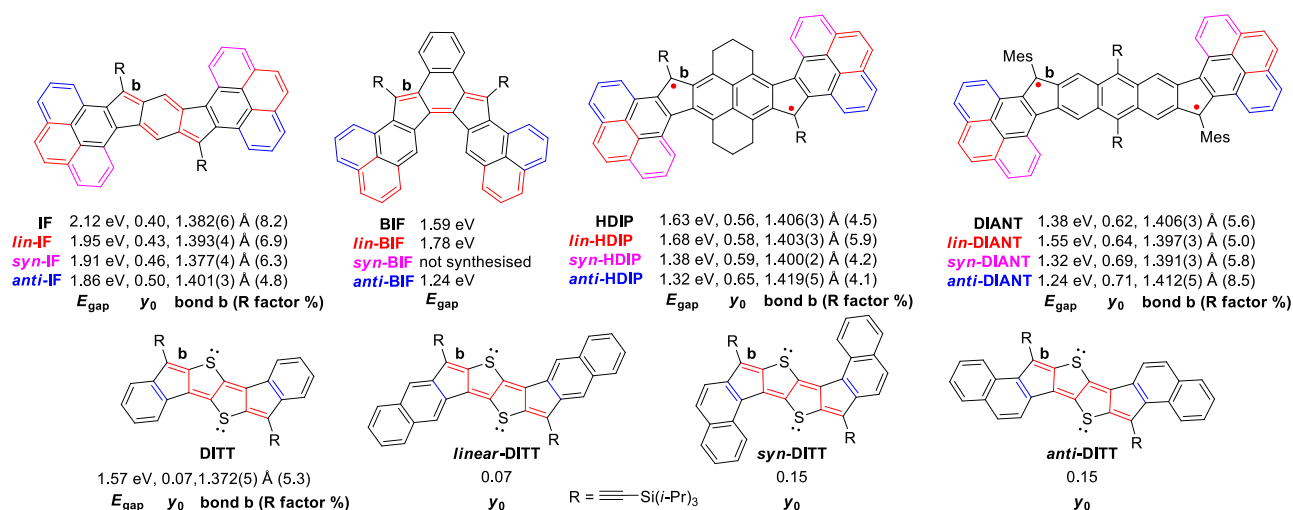


Fig. 1. Previous reported Indeno[1,2-*b*]fluorenes (**IFs**), Benzo-indeno[2,1-*c*]fluorenes (**BIFs**); Diindeno[1,2-*b*]fluorenes (**HDIPs**), Diindenoanthracenes (**DIANTs**) and Diindeno[1,2-*b*]thiophene derivatives (**DITTs**) described in this study. Energy band gap (E_{gap}), diradical character (y_0), X-ray bond length *b* and reliability factor (*R*) in % are provided.

the two extreme cases for **BIFs** was as high as 0.54 eV whereas a value roughly of 0.30 eV was observed for **IFs**, **HDIPs** and **DIANTs** (Fig. 1). To date, among all diindenoacenes reported, the **anti-BIF** is the unique closed-shell structure with an optical absorption beyond 1000 nm. Even though having suitable HOMO/LUMO energy levels to achieve balanced charge injection and transport for ambipolar behavior, the molecular structure of **anti-BIF** can't be useful to promote a suitable π - π stacking for efficient charge transport.⁹

Discovery of new molecules structurally isoelectronic to **IFs** with a good overlap of molecular orbitals in the solid state and tunable optical properties of **BIFs** could be critical of use to develop excellent ambipolar semiconductors. Therefore, we turned our attention to diindeno[1,2-*b*]thiophene derivatives (**DITTs**) (Fig. 1). **DITT** previously synthesised by Chi and Haley in separate work,⁵ possessing formally the dicyclopenta[*a,f*]naphthalene core, can be regarded as an extended *as*-indacene core with 16 π -electrons (4n) if two π -electrons are counted for each sulphur atom.¹⁵ Alternatively, if the sulphur atoms do not allow the occurrence of an efficient paratropic ring current inherent of 4n systems, **DITT** having one extra double bond at the centre, could be regarded as an extended version of **BIF**. In such case, **DITT** derivatives would have similar optoelectrochemical properties of **BIFs** with similar structures of **IFs**. The diradical character calculated from the electron occupancies of the frontier natural orbitals through the Yamaguchi's scheme (y_0) at UHF/6-311G(d,p) indicates that **DITTs** derivatives are nearly pure closed-shell compounds.¹⁶ Within this series, if again the *syn* derivative exhibits the shortest *b*-bond, it will highlight that the *b*-bond for diindenoacene diradicaloids with average diradical character depends on the contribution of the *b*-bond of the closed-shell resonance to a significant extent.

Herein, we disclose the synthesis, optoelectrochemical properties, X-ray crystal structure analysis and OFET properties

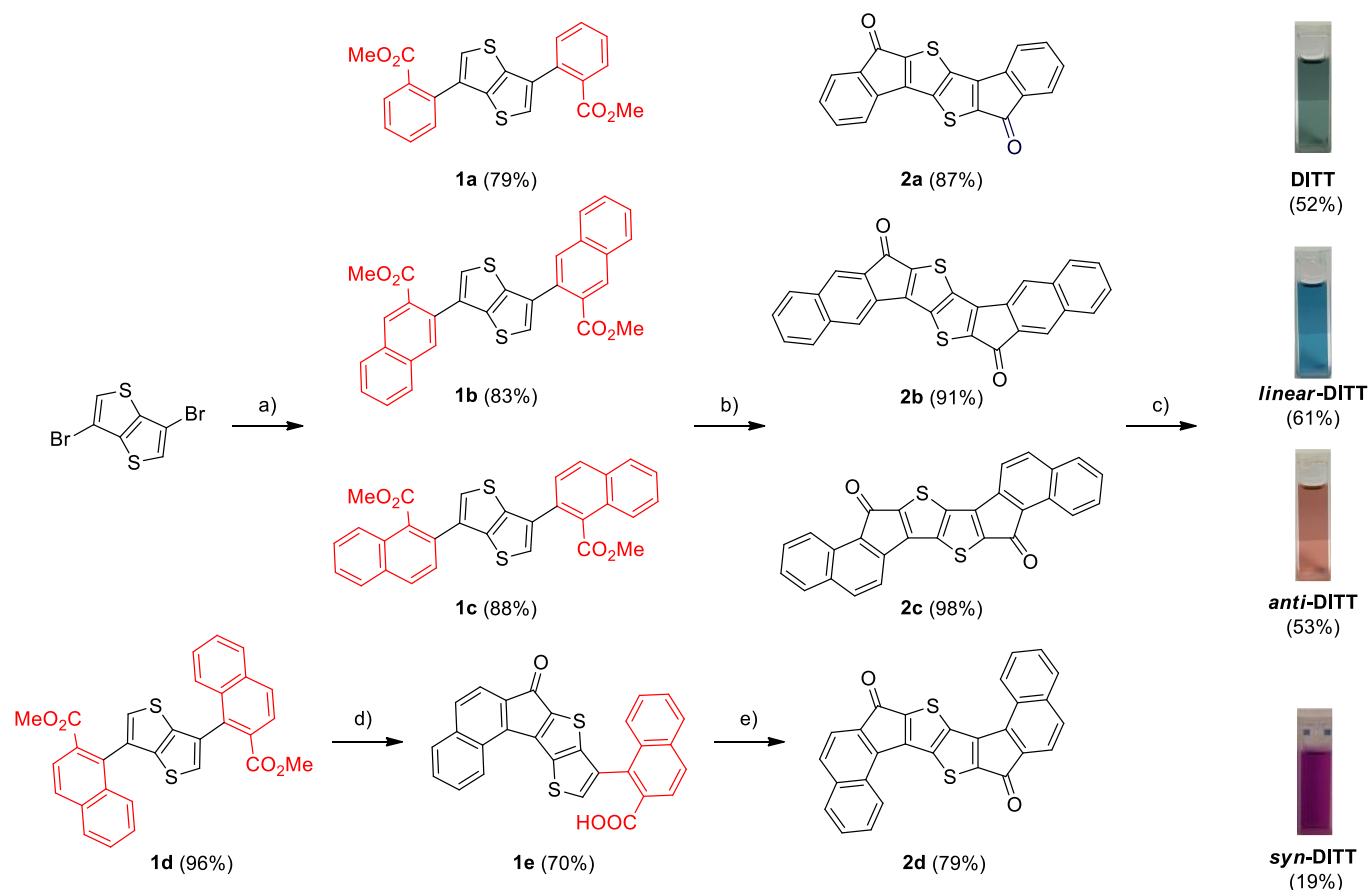
of **DITTs**. The tropicity of **DITTs** is discussed based on theoretical calculations such Nucleus-Independent Chemical Shift (NICS) and Anisotropy of the Induced Current Density (ACID) plot.

Results and discussion

Synthesis. The synthesis of **DITTs** is depicted in Scheme 1. They are obtained in three or four steps from 3,6-dibromothiopheno[3,2-*b*]thiophene. The first step involves the latter and boronic esters in a cross-coupling reaction providing diesters **1a–1d** in good yields. The double intramolecular Friedel-Crafts cyclisation using triflic acid as activator is efficient for **1a–1c** and give diketones **2a–2c** in excellent yields.¹⁷ However, starting from **1d**, the reaction didn't go to completion no matter the number of equivalents of triflic acid used. We assume that there is a rearrangement from 5-MR to 6-MR in the course of the reaction. The diketone **2d** is obtained in a sequential sequence instead. By using 7 equivalents of triflic acid, the monocyclised product was obtained in 70% yield and the remained ester function was then saponified in a quantitative yield to give compound **1e**. Chlorination of the acid then cyclisation using aluminium chloride furnishes diketone **2d** in 79%. All the diketones show the IR signature of an aromatic ketone of a 5-MR between 1700-1690 cm^{-1} (Supporting information). Finally, **DITTs** are obtained by first the nucleophilic attack of lithium-acetylide into the diones followed by the reductive reaction of the diol intermediates using tin chloride. It should be noted that the yields of **DITTs** are superior to 50% except for **syn-DITT** for which the yield is only 19%. The same trend has been observed for other diindenoacenes.^{7,8} However, it is difficult to provide any clear explanation on their reactivity.

X-ray structure analysis. Suitable single crystals of the four compounds for X-ray diffraction analyses were obtained. The X-ray bond lengths (in red) are depicted in Fig. 2 along with those calculated (in black) at R-B3LYP level of theory.¹⁸ All four

ARTICLE



compounds have a planar structure. However, in **anti-DITT**, the triple bonds deviate slightly from the plane of the π -conjugated backbone due to the steric repulsion between the triple bonds and the hydrogen at the zigzag edge of the fused-naphthalene. Consequently, the length of the a -bond is the longest for **anti-DITT** (1.490 Å). The X-ray structures clearly show that the compounds have a quinoid structure. Bond length alternation (BLA) between single and double bonds are observed across the π -conjugated spacer from the 5-MR to the central thienothiophene moiety. The main differences of the bond lengths are located in the 5-MR. The bond length b is the longest for **DITT** (1.372 Å) and **anti-DITT** (1.370 Å). It is the first time that both analogues have a very similar b -bond length and consequently this confirms that **DITT** derivatives are closed-shell structures. It should be noted that in all diindenoacene

diradicaloids reported to date, **anti**-derivatives have always the longest b -bond by far. This underlines that for **anti**-diradicals, the radicals delocalize more on the outer rings compared to their smaller analogues. The bond length b is the shortest for **syn-DITT** (1.362 Å) and **linear-DITT** has an intermediate value (1.365 Å). **HDIP** and **DIANT** diradicals have the same order regarding the bond length b highlighting that a shorter b -bond for diradicaloid with open-shell ground state is primarily due to a shorter b -bond of the closed-shell form. This finding gives a better understanding on the bond lengths of diindenoacene diradicaloids and is of great fundamental importance. Also, the bond length c at the fusion between the outer rings and the central core increases roughly about 0.02 Å considering that the bond length of perfect benzene is 1.390 Å and the bond lengths

ARTICLE

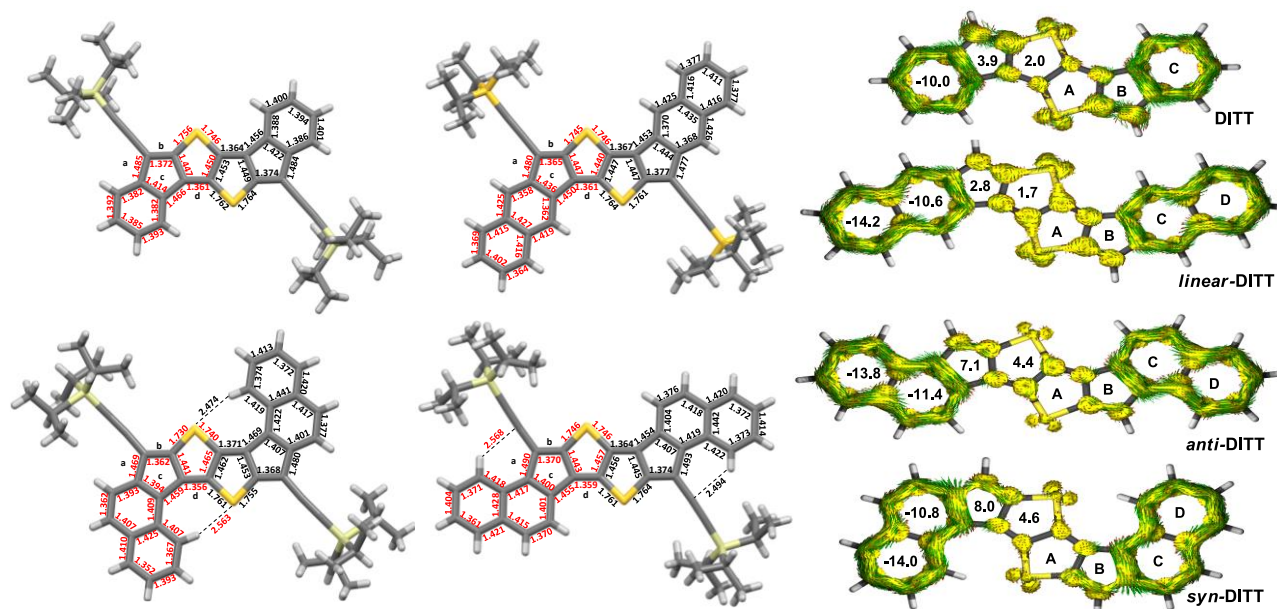


Fig. 2 X-ray bond lengths (red) with calculated bond lengths (black) at R-B3LYP, NICS (1.7) π_{zz} (inside the rings) and ACID plot for DITT derivatives.

of the 1,2 and 2,3 bonds in naphthalene are 1.374 and 1.416 Å, respectively.¹⁹

Tropicity calculations. In order to determine how DITT derivatives should be classified as either *as*-indacene core with 16 π -electrons or simply as quinoidal molecules bridged with two sulphur atoms, NICS(1.7) π_{zz} ²⁰ and ACID plot theoretical calculations were performed (Fig. 2).²¹ The NICS of the 5-MR and thienothiophene show small positive values which indicates that the inner rings are weakly antiaromatic. The paratropicity of the 5-MR is higher for *syn*- and *anti*-DITT due to a smaller bond length *c* at the fusion since the bond *c* should have a double bond character in a perfect $4n$ circuit. As one can see from the ACID plot, there is no clear paratropic ring current suggesting that the sulphur atoms with long C-S bonds prevent the occurrence of an efficient paratropic ring current in these systems. Consequently, DITT derivatives should be regarded as simple quinoid structures bridged with two sulphur atoms. The outer benzenoid rings show as expected diatropic ring currents. Compared to NICS values of benzene (−17.3 ppm) or naphthalene (−18.0 ppm), the NICS values are genuinely lower. For DITT, the benzene ring has a NICS value of only −10.0 ppm. This decreasing of the diatropicity can be ascribed to the bond lengths especially to the *c*-bond which is much longer than the bond length of a perfect benzene. The effect of the lengthen of the *c*-bond is also observed for the other derivatives. The benzenoid rings fused with the 5-MR have a NICS value of around −11 ppm which is lower than the external rings which

have a NICS value of −14 ppm. The diatropic ring current difference of the two rings is mainly due to the bond lengths and not to the paratropicity of the adjacent 5-MR since for IF derivatives for which the central core is more antiaromatic, the diatropicity of the external rings are similar.⁶

Optoelectrochemical properties. The optical properties were determined in toluene solution and the absorption spectra are given in Fig. 3a. Only the *linear*-DITT which has a central core the least antiaromatic, displays an intense absorption peak at 639 nm (λ_{max}) with a sharply decreasing shoulder at 676 nm. According to TD-DFT calculations (Table S5), this absorption is assigned to the symmetry-allowed S_0 - S_1 transition with a strong oscillator strength (f) of 1.05. *Linear*-DITT has an optical band gap of 1.69 eV. The absorption bands at 607 nm, 679 nm and 718 nm for DITT, *syn*- and *anti*-DITT respectively correspond to the symmetry-allowed S_0 - S_2 transitions with $f = 0.61$, 0.16 and 0.22, respectively. The values of f are fairly in agreement with the experimental data and are inversely correlated to the paratropicity of the central rings. Above the λ_{max} , a weak and broad absorption extended to 800 nm is observed for DITT and for *syn*- and *anti*-DITT, the absorption cut-offs are at 1000 nm and 1050 nm, respectively. These weak absorptions are assigned to the symmetry-forbidden S_0 - S_1 transition ($f = 0$). The values of the optical band gap are found to be 1.57, 1.38 and 1.30 eV for DITT, *syn*- and *anti*-DITT, respectively. The same trends were observed for BIFs derivatives.¹⁴ It should be noted that according to TD-DFT calculations (Table S6), IF derivatives

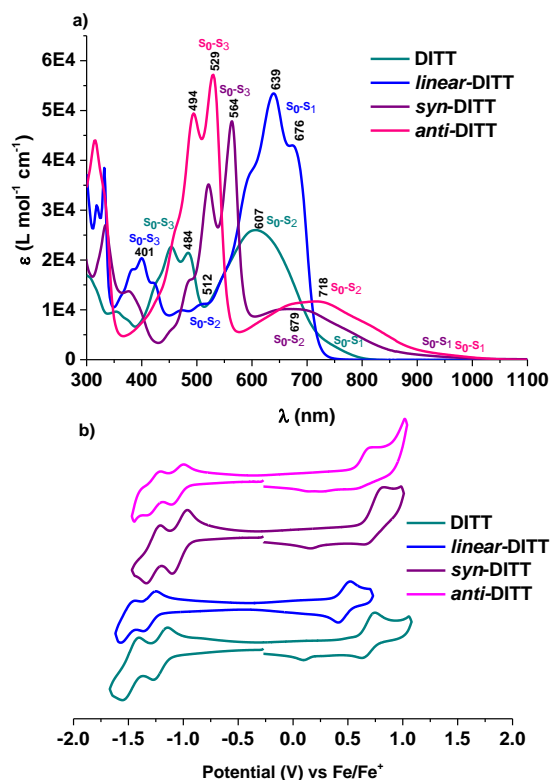


Fig. 3. Optical and electrochemical properties of DITTs: a) UV/vis spectra in toluene; b) CV in chlorobenzene with 0.1 M Bu₄N.PF₆ as the supporting electrode.

possess the same transitions versus annelation than DITT derivatives. However, contrary to DITT derivatives, the symmetry-forbidden S₀-S₁ transitions are completely extinguished for IF derivatives.⁶ This may be due to their stronger paratropicity.⁶

It is interesting to note that the purple colour of *syn*-DITT and the magenta for *anti*-DITT in solution are mainly related to the S₀-S₃ transition while the blue colour of *linear*-DITT originated from S₀-S₁ transition and the green colour of DITT comes from both S₀-S₁ and S₀-S₂ transitions.

Cyclic voltammetry (CV) was carried out in chlorobenzene solution, half-wave and onset potentials were determined relative to Fc/Fc⁺ couple (Fig. 3b and Table S1). All the compounds exhibit two reversible reduction peaks whereas only *linear*-DITT show a reversible oxidation peak. *Syn*- and *anti*-DITT for which the central core is the most antiaromatic, have less negative reduction peaks at -1.04 V and -1.05 V, respectively, whereas DITT and *linear*-DITT show more negative reduction peaks at -1.21 V and -1.31 V, respectively. On the contrary, *linear*-DITT for which the central core is the least antiaromatic, shows the lowest oxidation potential (onset) at 0.39 V while DITT, *syn*-DITT and *anti*-DITT have higher potentials at 0.60, 0.63 and 0.56 V, respectively. As expected, the bond order at the fusion (bond c in blue in Fig. 1) and annelation mode govern the redox potentials. *Syn*- and *anti*-DITT which have the highest bond order, reduce at lower potential whereas *linear*-DITT which has the lowest bond order, reduces at higher potential and oxidizes at lower potential. Indeed, the degree of aromaticity of cyclopentadienyl anion and

the antiaromaticity of the cyclopentadienyl cation explains the difference of the redox potentials to a great extent.

Molecular packing analyses (Fig. 4). All four compounds crystallize within a triclinic symmetry with a *P*-1 space group. DITT gives columnar packing whereas *linear*- and *syn*-DITT exhibit parallel 1D-slipped stacks which do not interact to each other. *Anti*-DITT shows pseudo 2D-brick wall motif. The molecule in red has a significant overlap with molecules in green while with the molecules in blue, there are two short contacts with a distance of 3.34 Å. It should be noted that since *linear*-DITT has a similar length in the main-axis of the molecule than *anti*-DITT, both should have given similar packing. This discrepancy is due the presence of solvent molecules in the crystals of *linear*-DITT.

It is interesting to note that the IF counterparts exhibit slightly different packing in the solid state.⁶ IF does not show any intermolecular interactions. *Linear*- and *anti*-IF show parallel 1D stacks whereas *syn*-IF shows 1D stacks with different orientations.

To gauge the strength of the intermolecular orbital interactions, transfer integrals for holes (t_n^{hole}) and electrons (t_n^{e}) of DITT derivatives were calculated at the Gaussian PW91 level of theory for all π -dimers within the stack (Fig. 4 and Table 1).²² For comparison purposes, these calculations were also done for IF derivatives and TIPS-pentacene (TIPS-PEN). Among DITT derivatives, *anti*-DITT exhibits the highest transfer integrals for both holes and electrons. Surprisingly, its hole transfer integral is 4 times higher than those of TIPS-PEN in the main transport direction. However, the values of the hole transfer integrals are weak for *linear*- and *syn*-DITT. On the contrary, the electron transfer integral for *linear*-DITT is large while the values are small for *syn*- and DITT. Even though *anti*-IF shows large transfer integrals for both holes and electrons, it only exhibits unipolar *p*-type semiconducting behavior while having a low lying LUMO energy level.¹³ Surprisingly, *linear*-IF which reported to possess a high OFET mobility ($1.04 \pm 0.68 \text{ cm}^2 \text{ V}^{-1} \text{ s}^{-1}$) exhibited a very low hole transfer integral (5.4 meV).¹³ *Anti*-IF has a hole transfer integral about 16 times stronger than that of *linear*-IF and exhibited a hole mobility of $4.72 \pm 1.97 \text{ cm}^2 \text{ V}^{-1} \text{ s}^{-1}$.¹³ The drift mobilities for these molecules were also calculated based on the classical Marcus-Hush theory and summarized in Table 1, which basically follow the degrees of the transfer integrals. However, the mobilities of DITT derivatives are expected to be not very high because of large reorganization energies.

OFET devices. The charge transport properties of DITT derivatives were experimentally investigated by fabricating OFET devices with bottom-gate/top-contact (BG/TC) configuration. The active layer of DITT derivatives were formed by drop-casting from *o*-dichlorobenzene at 60°C. Surprisingly, the obtained mobilities showed a quite different tendency from the theoretically calculated values. The DITT derivatives showed bipolar transport except *linear*-DITT as shown in Fig. 5 and Table 1 although the calculated electron mobility for *linear*-DITT was higher than those obtained for the other derivatives. This may be attributed to the higher LUMO energy level resulting in a large injection barrier and no gate effect. On the other hand,

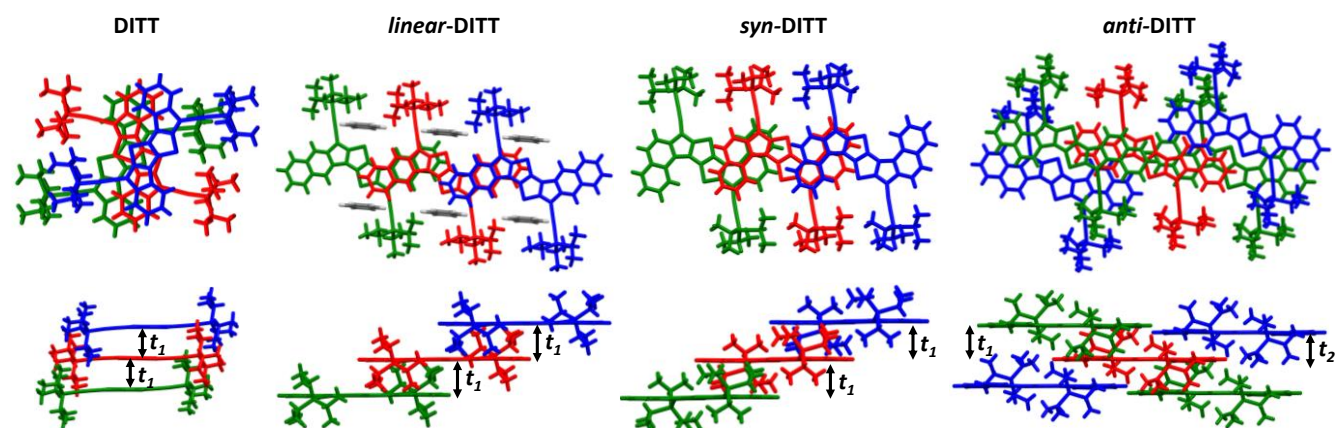


Fig. 4. Molecular Packing of DITT derivatives.

Table 1. Calculated transfer integrals, reorganization energies, and mobilities for holes and electrons for **DITTs**, **IFs** and **TIPS-PEN** and OFETs characteristics of **DITT** derivatives and **linear-IF**.

Compounds	Theoretical								Experimental			
	$t_1^{\text{hole[a]}}$	$t_2^{\text{hole[a]}}$	$\lambda_h^{\text{[b]}}$	$\mu^{\text{hole[c]}}$	$t_1^{\text{e-[a]}}$	$t_2^{\text{e-[a]}}$	$\lambda_e^{\text{[b]}}$	$\mu^{\text{e-[c]}}$	$\mu^{\text{hole[c]}}$	V_{th} (V)	$\mu^{\text{e-[c]}}$	V_{th} (V)
DITT	72.1	/	147	4.9×10^{-1}	17.7	/	336	3.0×10^{-3}	3.1×10^{-3}	-52	3.6×10^{-4}	33
linear-DITT	1.4	/	119	1.0×10^{-3}	60.6	/	289	3.6×10^{-1}	1.1×10^{-4}	-34	No gate effect	
syn-DITT	9.3	/	234	1.2×10^{-2}	-16.1	/	319	1.4×10^{-2}	1.5×10^{-3}	-56	1.6×10^{-2}	59
anti-DITT	-99.9	-16.1	230	5.6×10^{-1}	-69.2	-1.7	339	2.5×10^{-1}	2.5×10^{-4}	-58	1.0×10^{-4}	55
IF	/	/	202	2.5×10^{-2}	/	/	250	2.0×10^{-3}				
linear-IF	5.4	/	153	1.2×10^{-2}	-34.9	/	248	1.7×10^{-1}	7.0×10^{-4} $1.04 \pm 0.68^{\text{[d]}}$	-56	7.2×10^{-5}	40
syn-IF	-85.0	/	195	1.75	42.5	/	227	3.0×10^{-1}				
anti-IF	80.1	/	246	8.3×10^{-1}	-84.6	/	211	1.4	$4.72 \pm 1.97^{\text{[d]}}$			
TIPS-PEN	23.8	-2.80	119	3.2×10^{-1}	-129.6	-63.5	170	4.3				

[a] Transfer integrals in meV. [b] Charge reorganization energy in meV. [c] Mobility in $\text{cm}^2 \text{V}^{-1} \text{s}^{-1}$. [d] Taken from ref. 13.

syn-DITT with a lower LUMO level showed a good electron mobility. In addition, **linear-IF** having moderate γ_0 value, in our hands, was found to show a bipolar transport although the hole mobility was four order of magnitude lower than the reported value (Table 1).¹³ Some recent works also revealed that the compounds with an open-shell nature, have a high potential to lead a good ambipolar OFET, while **DITT** derivatives may give an additional insight to the charge transport of organic semiconductors since they have closed-shell structures.^{3c,d} Both hole and electron mobilities of **anti-DITT** were unfortunately lower than those expected from the theoretical calculation, which is due to a poor film quality caused by a strong aggregation (Fig. S5).

In addition, the large reorganization energies of these compounds may limit the efficient charge carrier transport.

Conclusions

Four diindenothiophene (**DITTs**) derivatives have been synthesised. The bond lengths analysis highlights that **DITTs** are closed-shell structures in agreement with the calculated diradical character. In addition, this analysis brings insight on the apical bond length of 5-MR to the central core observed in diindenoacene diradicaloids. **DITTs** are molecules with low band gap ranging from 1.69 to 1.30 eV. While having formally an extended *as*-indacene core with 16 π -electrons, they should be considered as quinoidal skeleton bridged with 2 sulphur atoms. The optoelectrochemical properties are close to benzo-fused indeno[2,1-*c*]fluorenes (**BIFs**). **DITTs** and **BIFs** are both quinoidal molecules. The annelation mode of the outer rings governs the

optoelectrochemical properties, the tropicity and the packing in the solid phase. Their performances in thin film OFETs were evaluated demonstrating ambipolar behaviours.

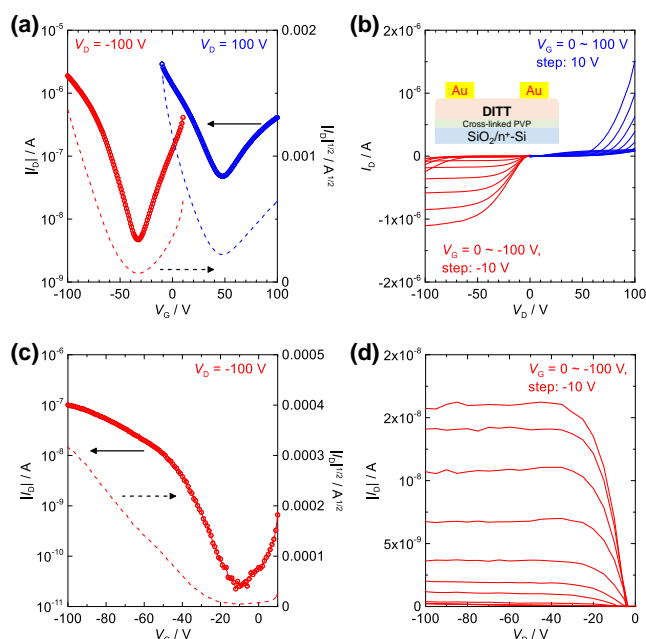


Fig. 5. OFET device of DITT derivatives. (a) Transfer and (b) output characteristics of DITT. (c) Transfer and (d) output characteristics of linear-DITT. The OFET characteristics for *syn*-DITT and *anti*-DITT are shown in Fig. S3.

Conflicts of interest

There are no conflicts to declare.

Acknowledgements

M.F. and A.Y. acknowledge financial support from the Agence Nationale de la Recherche ANR-16-CE07-0024 (GATE). M.M. acknowledges financial support from JSPS KAKENHI Grant Number 19H02790, 20K21227 and 21H05401, Inamori Foundation, Iketani Science and Technology Foundation, and JSPS Core-to-Core Program (JPJSCA20180005).

References

- 1) a) M. Bendikov, F. Wudl and D. F. Perepichka, *Chem. Rev.*, 2004, **104**, 4891-4946; b) J. E. Anthony, *Angew. Chem. Int. Ed.*, 2008, **47**, 452-483; *Angew. Chem.* 2008, **120**, 460-492; c) Q. Ye, C. Chi, *Chem. Mater.*, 2014, **26**, 4046-4056.
- 2) a) J. Roncali, P. Leriche and P. Blanchard, *Adv. Mater.*, 2014, **26**, 3821-3838; b) A. Naibi Lakshminarayana, A. Ong and C. Chi, *J. Mater. Chem. C*, 2018, **6**, 3551-3563; c) J.-Y. Shin, T. Yamada, H. Yoshikawa, K. Awaga and H. Shinokubo, *Angew. Chem. Int. Ed.*, 2014, **53**, 3096-3101.
- 3) a) J. Mei, Y. Diao, A. L. Appleton, L. Fang and Z. Bao, *J. Am. Chem. Soc.*, 2013, **135**, 6724-6746; b) G. Schweicher, G. Garbay, R. M. Jouclas, F. Vibert, F. I. Devaux and Y. H. Geerts, *Adv. Mater.*, 2020, **32**, 1905909; c) S. Dong and Z. Li, *J. Mater. Chem. C*, 2022, **10**, 2431-2449; d) T. Higashino and T. Mori, *Phys. Chem. Chem. Phys.*, 2022, DOI : 10.1039/D1CP05799E.
- 4) a) J. J. Dressler and M. M. Haley, *J. Phys. Org. Chem.*, 2020, **33**, e4114; b) C. K. Frederickson, B. D. Rose and M. M. Haley, *Acc. Chem. Res.*, 2017, **50**, 977-987.
- 5) a) X. Shi, P. M. Burrezo, S. Lee, W. Zhang, B. Zheng, G. Dai, J. Chang, J. T. Lopez Navarrete, K.-W. Huang, D. Kim, J. Casado and C. Chi, *Chem. Sci.*, 2014, **5**, 4490-4503; b) G. E. Rudebusch, A. G. Fix, H. A. Henthorn, C. L. Vonnegut, L. N. Zakharov and M. M. Haley, *Chem. Sci.*, 2014, **5**, 3627-3633.
- 6) C. K. Frederickson, L. N. Zakharov and M. M. Haley, *J. Am. Chem. Soc.*, 2016, **138**, 16827-16838.
- 7) T. Jousselein-Oba, M. Mamada, A. Okazawa, J. Marrot, T. Ishida, C. Adachi, A. Yassar and M. Frigoli, *Chem. Sci.*, 2020, **11**, 12194-12205.
- 8) J. J. Dressler, A. Cardenas Valdivia, R. Kishi, G. E. Rudebusch, A. M. Ventura, B. E. Chastain, C. J. Gomez-Garcia, L. N. Zakharov, M. Nakano, J. Casado and M. M. Haley, *Chem*, 2020, **6**, 1353-1368.
- 9) K. Sbagoud, M. Mamada, J. Marrot, S. Tokito, A. Yassar and M. Frigoli, *Chem. Sci.*, 2015, **6**, 3402-3409.
- 10) a) G. E. Rudebusch, J. L. Zafra, K. Jorner, K. Fukuda, J. L. Marshall, I. Arrechea-Marcos, G. L. Espejo, R. Ponce Ortiz, C. J. Gómez-García, L. N. Zakharov, M. Nakano, H. Ottosson, J. Casado and M. M. Haley, *Nat. Chem.*, 2016, **8**, 753-759; b) D. T. Chase, A. G. Fix, S. J. Kang, B. D. Rose, C. D. Weber, Y. Zhong, L. N. Zakharov, M. C. Lonergan, C. Nuckolls, M. M. Haley, *J. Am. Chem. Soc.*, 2012, **134**, 10349-10352.
- 11) Y.-C. Hsieh, C.-F. Wu, Y.-T. Chen, C.-T. Fang, C.-S. Wang, C.-H. Li, C.-H. L.-Y. Chen, M.-J. Cheng, C.-C. Chueh, P.-T. Chou and Y.-T. Wu, *J. Am. Chem. Soc.*, 2018, **140**, 14357-14366.
- 12) J. Melidonie, E. Dmitrieva, K. Zhang, Y. Fu, A. A. Popov, W. Pisula, R. Berger, J. Liu and X. Feng, *J. Org. Chem.*, 2020, **85**, 215-223.
- 13) A. M. Zeidell, L. Jennings, C. K. Frederickson, Q. Ai, J. J. Dressler, L. N. Zakharov, C. Risko, M. M. Haley and O. D. Jurchescu, *Chem. Mater.*, 2019, **31**, 6962-6970.
- 14) T. Jousselein-Oba, P. E. Deal, A. G. Fix, C. K. Frederickson, C. L. Vonnegut, A. Yassar, L. N. Zakharov, M. Frigoli and M. M. Haley, *Chem. Asian J.*, 2019, **14**, 1737-1744.
- 15) a) T. Xu, Y. Han, Z. Shen, X. Hou, Q. Jiang, W. Zeng, P. W. Ng and C. Chi, *J. Am. Chem. Soc.*, 2021, **143**, 20562-20568; b) J. E. Barker, C. K. Frederickson, M. H. Jones, L. N. Zakharov and M. M. Haley, *Org. Lett.*, 2017, **19**, 5312-5315.
- 16) a) D. Doehnert and J. Koutecky, *J. Am. Chem. Soc.*, 1980, **102**, 1789-1796; b) K. Yamaguchi, T. Kawakami, Y. Takano, Y. Kitagawa, Y. Yamashita and H. Fujita, *Int. J. Quantum Chem.*, 2002, **90**, 370-385.
- 17) a) T. Jousselein-Oba, M. Mamada, K. Wright, J. Marrot, C. Adachi, A. Yassar and M. Frigoli, *Angew. Chem. Int. Ed.* 2022, **61**, e202112794; *Angew. Chem.* 2022, **134**, e202112794; b) T. Jousselein-Oba, M. Mamada, J. Marrot, A. Maignan, C. Adachi, A. Yassar and M. Frigoli, *J. Am. Chem. Soc.*, 2019, **141**, 9373-9381; c) K. Sbagoud, M. Mamada, T. Jousselein-Oba, Y. Takeda, S. Tokito, A. Yassar, J. Marrot and M. Frigoli, *Chem. Eur. J.*, 2017, **23**, 5076-5080.
- 18) Deposition Numbers 2159650-2159653 contain the supplementary crystallographic data for this paper. These data are provided free of charge by the joint Cambridge Crystallographic Data Centre and Fachinformationszentrum Karlsruhe Access Structures service www.ccdc.cam.ac.uk/structures.
- 19) J. Oddershede and S. Larsen, *J. Phys. Chem. A*, 2004, **108**, 1057-1063.
- 20) a) A. Stanger, *J. Org. Chem.*, 2010, **75**, 2281-2288; b) R. Gershoni-Poranne and A. Stanger, *Chem. Eur. J.*, 2014, **20**, 5673-5688.
- 21) R. Herges and D. Geuenich, *J. Phys. Chem. A*, 2001, **105**, 3214-3220.

22 W.-Q. Deng and W. A. Goddard, *J. Phys. Chem. B*, 2004, **108**, 8614-8621.